Spatio-Temporal Distributions of the Natural Non-Sea Salt Aerosol over the Southern Ocean and Coastal Antarctica and its Potential Source Regions

Information about the database, details of data processing, and complementary results

Jost Heintzenberg et al.

1. Information about the database

In Table T1 the logistic data of the sites and cruises are compiled together with relevant citations. The map in Figure S1 shows the cruise tracks of all utilized experiments and the locations of the stations used in the present study. Only samples and hourly CPC-data are considered with air-ass back trajectories not touching any continent north of Antarctica within five days before arrival at the measuring point. After trajectory-filtering 19205 samples remained comprising 788545 sampling hours. The corresponding number of filtered sampling hours of CPC-data was 331747. In Figure S2 the meridional distribution of data chemical aerosol samples and hourly CPC-data are collected from all sites and research cruises of the present study. To make the sample events comparable to the hourly CPC-values the occurrences in each latitudinal bin were divided by the total

number in each distribution. In both subsets of the database Antarctic coastal stations dominate the meridional distributions. Only the long CPC-timeseries at Kennaook Cape Grim Tasmania yields a secondary data maximum with 19% of the data.

Table T1 Names of stations or experiments (cruise names in caps), station acronyms, station coordinates (S.O. = Southern Ocean parts of cruises, N_3 = time periods with number concentrations of particles > 3 nm, N_{10} = time periods with number concentrations of particles > 10 nm, Major ions= time periods with samples in which the particulate chemical components Na, NH_4, K, Mg, Ca, MSA, Cl, NO_3, SO_4 were analyzed, Citations = relevant publications concerning the data used in the present study, (PC = Personal Communication).

Station or Experiment	**Station acronym**	**Latitude**	**Longitude**	**N_3**	**N_{10}**	**Major ions**	**Citations**
Aboa, Antarctica	ABO	-73.05	-13.42	2006-12-29_2007-1-29	2006-12-29_2007-1-29	1998-01-01_1998_02_02, 2006-12-30_2007-01-28	(Teinilä et al., 2000), (Asmi et al., 2010)
ACADEMIC FEDOROV 1999		S.O.	S.O.	1999-11-08_1999-12-08	1999-11-08_1999-12-08	1999-11-08_1999-12-08	(Koponen et al., 2002)
ACE (Antarctic Circumnavigation Expedition)		S.O.	S.O.		2016-12-20_2017-03-30	2016-12-20_2017-03-21	(Schmale et al., 2019a),

							(Schmale et al., 2019b)
ACE1_DISCOVERER		S.O.	S.O.	1995-10-13_1995-12-12	1995-10-13_1995-12-12	1995-10-26_1995-12-11	(Bates et al., 2000)
AEROSOLS99		S.O.	S.O.	1999-01-28_1999-02-24	1999-01-28_1999-02-24	1999-01-28_1999-02-24	(Bates et al., 2001)
Amsterdam Island	AMI	-37.48	77.34			2003-05-02_2011-12-26 2006-12-03_2007-04-05	(Claeys et al., 2010)
ANA06B		S.O.	S.O.			2016-01-07_2016-02-22	(Jung et al., 2020)
Arctowski, Antarctica	ARC	-62.15	-58.42		2013-03-01_2013-10-31		(Kubicki et al., 2016)
Baring Head, New Zealand	BAH	-41.42	174.87			1993-08-23_1996-11-05 2015-07-07_2016_08-04	(Savoie and Prospero, 1989), (Li et al., 2018)
Bird Island	BDI	-54.01	-38.05		2010-11-17_2010-12-28	2010-11-03_2010-12-26	(Schmale et al., 2013)
Kennaook Cape Grim, Tasmania	CGI	-40.68	144.69		1989-2020	1976-2010	(Savoie and Prospero, 1989;

							Gras, 1990; Gras, 1995; Ayers et al., 1996; Ayers et al., 1997; Ayers and Gillett, 2000; Keywood, 2003)
Cape Point, South Africa	CPT	-34.35	18.49		2008-01-01_2013-12-31		PC
CAPRICORN1		S.O.	S.O.	2016-03-14_2016-04-15		2016-03-14_2016-03-25	(Humphries et al., 2021)
CAPRICORN2		S.O.	S.O.		2018-01-10_2018-02-21	2018-01-14_2018-02-21	(Humphries et al., 2021)
Chatham Island	CHI	-43.92	-176.50			1983-09-15_1996-10-04	(Savoie, 1984)
CHINARE		S.O.	S.O.			2014-02-02_2014-04-14	(Zhang et al., 2021)
Davis, Antarctica	DAV	-68.58	77.97			1988-11-18_1991-02-23	3359
Dumont d'Urville, Antarctica	DDU	-66.67	140.02			1991-03-01_2017-10-15	(Weller et al., 2011b; Legrand

							et al., 2016; Legrand et al., 2021)
Falkland Island	FAI	-51.75	-60.00			1987-07-23_1996-18-11	(Savoie and Prospero, 1989)
G.v.Neumayer, Antarctica	GVN	-70.67	-8.27	1996-2021	1993-2018	1983-2021	(Weller et al., 2008; Weller et al., 2011a; Weller et al., 2011b; Weller et al., 2015)
King George Island	KGI	-62.18	-58.30			1990-03-27_1996-09-19	(Savoie et al., 1993)
King Sejong, Antarctica	KSJ	-62.22	-58.78	2009-2019	2009-2019	2013-01-13_2014-01-11, 2019-01-17_2020-01-24	(Hong et al., 2020; Jang et al., 2022)
MacMurdo, Antarctica	MAM	-77.85	166.73		2015-11-15_2017-01-03		(Lubin et al., 2020)
Macquarie Island	MAI	-54.50	158.95	1995-11-21_1995-12-12	1995-11-21_1995-12-12	1988-12-09_1993-03-03,	(Brechtel et al.,

						1995-10-31_1995-12-26	1998)
Maitri, Antarctica	MAT	-70.77	11.73		2005-01-01_2005-02-27		(Pant et al., 2011)
Marambio, Antarctica	MAR	-64.25	-56.63			2013-02-07_2015-11-30	(Asmi et al., 2018)
MARCUS		S.O.	S.O.		2017-10-29_2018-03-24		(McFarquhar et al., 2021)
Mario Zucchelli, Antarctica	MAZ	-74.68	164.10			2010-11-29_2011-01-23, 2014-11-06_2015-01-13	(Becagli et al., 2022)
Marion Island	MRI	-46.92	37.75			1992-02-25_1996-01-01	(Savoie and Prospero, 1989)
Mawson, Antarctica	MAW	-67.60	62.50			1987-02-18_1996-01-01	(Savoie et al., 1993), (Prospero et al., 1991; Savoie et al., 1992)
NORTHWIND		S.O.	S.O.		1979-12-18_1980_01-04		(Hogan, 1981)
OAC92		S.O.	S.O.		1992-11-14_1993-01-03	1992-11-14_1993-01-03	(Leck et al., 2002)

OOMPH2007		S.O.	S.O.			2007-01-19_2007-03-23	(Zorn et al., 2008)
Palmer, Antarctica	PAL	-64.77	-64.05			1990-04-03_1996-10-12	(Savoie et al., 1993)
PEGASO		S.O.	S.O.		2015-01-05_2015-02-07	2015-01-05_2015-02-08	(Decesari et al., 2020)
POLARSTERN		S.O.	S.O.		2011-04-23_2011-05-17, 2011-10-29_2011-11-29, 2012-04-13_2012-05-12, 2012-10-28_2012-11-26	2011-04-23_2011-05-17, 2011-10-29_2011-11-29, 2012-04-13_2012-05-12, 2012-10-28_2012-11-26	(Huang et al., 2018)
Princess Elisabeth, Antarctica	PRE	-71.95	23.35	2012-2019			(Herenz et al., 2019)
Russian Antarctic Expeditions		S.O.	S.O.			2004-2019	(Sakerin et al., 2022)
RITS93		S.O.	S.O.	1993-03-21_1993-05-07	1993-03-21_1993-05-07	1993-03-22_1993-05-06	(Quinn et al., 2017)
RITS94		S.O.	S.O.	1993-11-21_1994_01-07	1993-11-21_1994_01-07	1993-12-05_1994-01-05	(Quinn et al., 2017)
SHIRASE		S.O.	S.O.		2011-2020		PC

SIPEX_II		S.O.	S.O.	2012-09-13_2012-11-15	2012-09-13_2012-11-15		(Humphries et al., 2016)
Syowa, Antarctica	SYO	-69.00	39.58		1997-05-01_2021-12-31		(Hara et al., 2019)
Wellington, New Zealand	WEZ	-41.28	174.78			1987-10-20_1993-08-23	(Savoie and Prospero, 1989)
XUELONG		S.O.	S.O.			2017-12-02_2018-02-14	(Yan et al., 2020; Wang et al., 2021)
Zhongshan, Antarctica	ZHO	-69.37	76.37			2005-02-01_2008-11-09	(Xu et al., 2019)

Table T2 Statistics of particle number concentrations (cm^{-3}), and major ion concentrations (ngm^{-3}) during the months October through April over the Southern Ocean and at island and coastal stations in Table S1. Non-sea-salt fractions are denoted as "nss". Only data with 5-day back trajectories not touching any continent are included.

Parameter	N_3	N_{10}	N_{3-10}	Na	NH_4	K	Mg	Ca	MSA	Cl	NO_3	SO_4	$nssSO_4$	nssK	nssMg	nssCa
Number of cases	99344	140900	26555	11483	13112	10463	5589	5247	13124	10103	13767	13737	11815	10396	5568	5224
Average	517	491	70	482	91	30	53	36	49	799	38	358	207	16	7.1	17
Standard deviation	488	426	161	945	125	71	182	178	65	1417	50	417	190	35	20	79
Median	386	382	26	167	39	11	19	7.3	29	267	26	229	165	1.7	0.93	0.73
Median absolute deviation	169	150	26	124	33	8.9	15	5.8	18	210	17	116	85	1.7	0.93	0.73

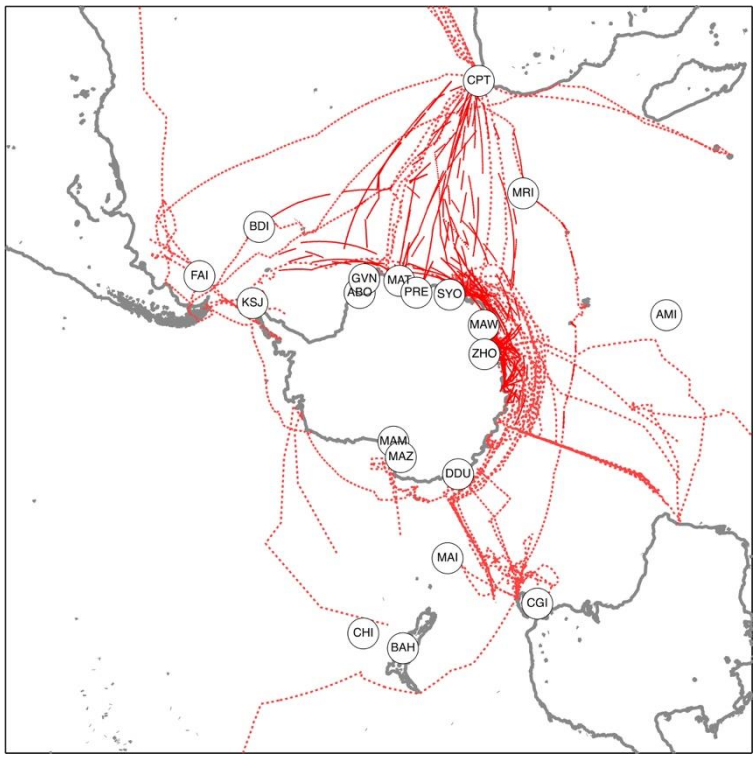

Figure S1 Stations and tracks of cruises used in the present study. Station acronyms are listed in Table S1. Only stations with non-overlapping marker-text are shown. For the Russian Antarctic Expeditions, only sampling periods are available.

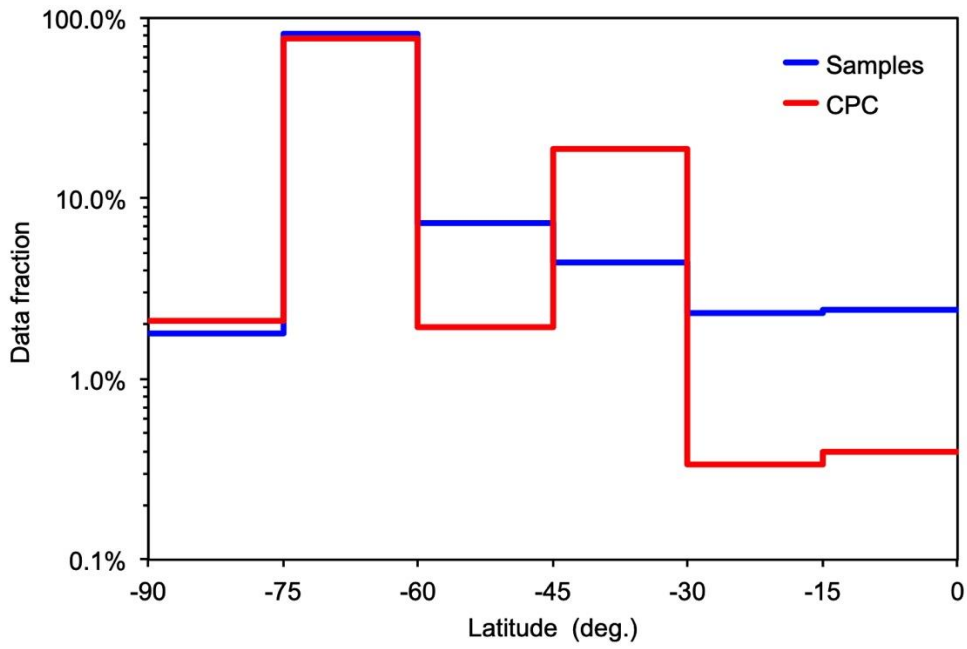

Figure S2 Relative meridional distributions of aerosol sample and CPC data points used in the present study. Only samples and hourly CPC-data are considered with back trajectories not touching any continent north of Antarctica within five days before arrival at the measuring point.

2. The problem of non-sea salt sulfate

At Kennaook Cape Grim, Tasmania very few samples were taken without any influence from the nearest continent. In Figure S3 this is illustrated for sulfate that shows high SO_4-values throughout the year with only a small indication of a potentially biogenic summer peak. The component $nssSO_4$ (NSSraw in Figure S3) exhibits a stronger seasonal variation albeit still considerably weaker than the purely biogenic component MSA, which we interpret as due to continental contamination, in particular during winter. As we were interested in the biological source of $nssSO_4$ we assumed that this component has a similar seasonal distribution as MSA and formulated a correction procedure based on the seasonal distribution of the latter and the potential continental contamination of the individual samples. The latter was calculated by the ratio of sampling hours with five-day back trajectories reaching a continent divided by the total number of sampling hours, termed BFRAC. For each month a correction term was calculated. This term was weighed by BFRAC of the individual samples and subtracted from NSSraw of the individual chemical aerosol samples in order to fit the seasonal variation of $nssSO_4$ to that of MSA while allowing for higher absolute values of $nssSO_4$ than for MSA by means of a scale factor. The 12 monthly correction terms plus the scale factor were determined with Excels General Reduced Gradient solver by fitting the corrected monthly median $nssSO_4$ values to the relative seasonal distribution of MSA. The results of this procedure are shown as NSSfit in Figure S3. The optimized scale factor was determined to MSA/NSSfit=0.28, which is somewhat higher than the value 0.23 given earlier in Ayers et al. (1996) for Kennaook Cape Grim.

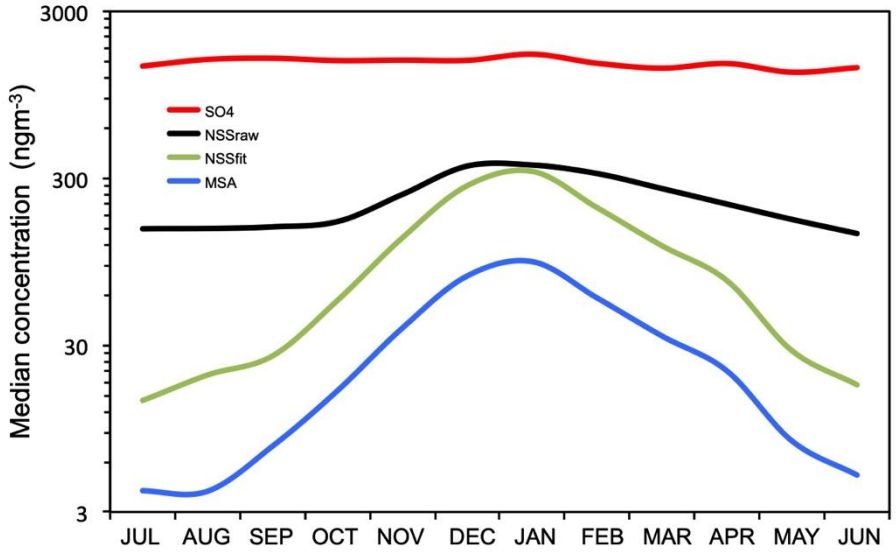

Figure S3 Monthly median sulfate (SO4), methane sulfonic acid distribution (MSA), raw monthly median $nssSO_4$ (NSSraw), and contamination-corrected median $nssSO_4$ (NSSfit) in ngm^{-3} from samples taken at Kennaook Cape Grim, Tasmania 1976-2008.

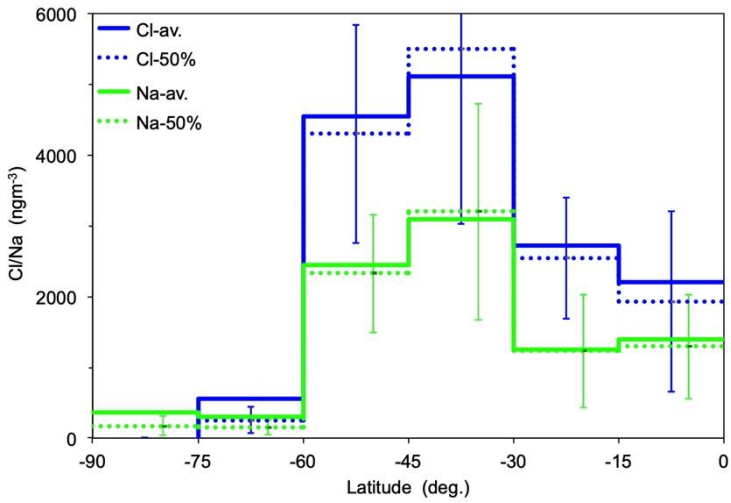

Figure S4 Annual average and median meridional distributions of Cl and Na over the Southern Ocean. Error bars correspond to median absolute deviations from the medians.

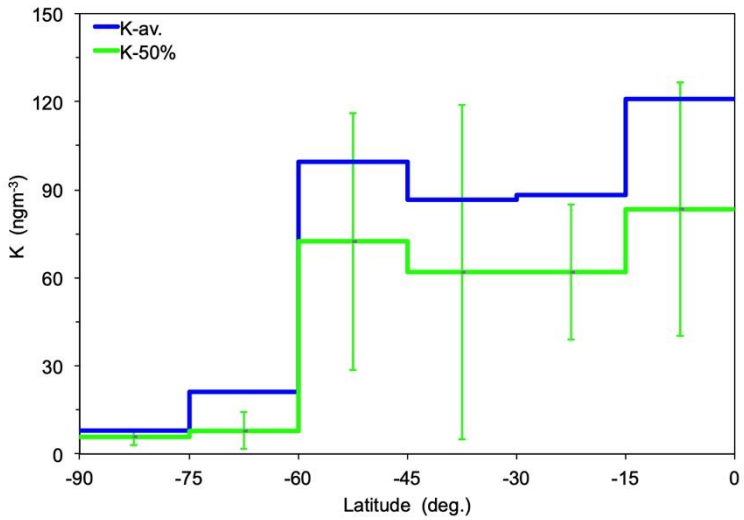

Figure S5 Annual average and median meridional distributions of K over the Southern Ocean. Error bars correspond to median absolute deviations from the medians.

4 Trajectory analysis

Hourly ten-day air-mass back trajectories were calculated arriving at 300 m over the sampling points. The trajectories cover each hour of the collected physical and chemical aerosol data. The trajectories were based on the meteorological fields kindly made available by the US National Weather Service's National Center for Environmental Prediction (NCEP). Post2005 the calculations were based on the Global Data Assimilation System (GDAS1). In horizontal grids of $1° \times 1°$ resolution, meteorological parameters are stored every three hours with a vertical grid spacing of 23 pressure surfaces between 1000 and 20 hPa. Vertical layers 1-5 are separated by 25 hPa. All higher layers (with the exception of the top layer) are separated by 50 hPa, (Kanamitsu, 1989). Before 2005 the trajectories are based on NCEP/NCAR reanalyzed meteorological fields with $2.5° \times 2.5°$ resolution (https://www.ready.noaa.gov/gbl_reanalysis.php, last accessed 2021-11-29). The HYSPLIT-model for trajectory calculation (Stein et al., 2015) analyzes the meteorological inputs to determine the appropriate internal vertical model resolution so that there are sufficient levels

to interpolate all the meteorological input without skipping data due to insufficient vertical resolution.

4 The problem of local and distant continental contamination

Any sampling of the natural aerosol in the pristine environment of the Southern Ocean or on Antarctica faces a high risk of contamination. This risk is at least twofold, beginning with local contamination since in most cases the necessary energy for the sampling instrumentation has to come through local combustion sources. These combustion sources emit high amounts of aerosol that needs to be minimized in the samples. At different stations and during different research cruises varying approaches have been used to avoid local contamination such as post-sampling inspection of results to eliminate outliers, often undocumented.

Wind sector controls, sometimes combined with windspeed thresholds reduce the risk of local contamination. Because of the proximity of the Australian mainland the Kennaook Cape Grim baseline station established early on such a baseline wind sector (Robbins and Enting, 1989) that is applied to particle number data at Cape Point and for part of the Kennaook Cape Grim data of the present study. At Cape Point and G.v.Neumayer a post-fact critical wind sector for local contamination was available from information in the literature or through discussion with the site operators, and was utilized in the present study. In these cases, a "local" wind direction was calculated from the back trajectories during the last hour before arriving at the sampling site. This wind direction was utilized in a virtual sector control, i.e. to eliminate samples as potentially locally contaminated. Much more rigorous sampling control is reached with fast sensitive condensation particle counters switching samplers off when set thresholds or temporal concentration changes are reached (e.g., Ogren and Heintzenberg, 1990).

The particular sampling conditions at the Australian Baseline station at Kennaook Cape Grim, Tasmania caused a contamination of chemical aerosol samples with local soil dust,

which was corrected with the help of local soil composition measurements according to the method detailed in Ayers (2001) and Keywood (2007).

Excluding distant aerosol sources that are not part of the present study is more difficult to achieve. Neff and Bertler (2015) quantified the contributions of continental dust sources to the aerosol over the Southern Ocean by means of a large ensemble of forward trajectories from the adjacent continents. The present synopsis is directed at the natural aerosol originating over the Southern Ocean, and the influence of surrounding continents has been minimized. For this purpose, hourly 10-day back trajectories to the available sampling stations and ships were utilized in an inverse way in this study, compared to the study of Neff and Bertler (2015). Whenever any such trajectory came within 10 km of any continental margin, (except for Antarctica), the travel time to the respective sampling site was noted, yielding a means to eliminate the data from any statistics.

A first test of this approach of minimizing any continental influence on the aerosol data of the present study to build on hourly values of N_3 and N_{10} taken at all sites and cruises and the travel times of their respective back trajectories to the nearest continents. In Figure S6 median N_3 and N_{10} as a function of travel time greater than three hours are plotted. From median values beyond 2000 cm^{-3} concentrations drop rapidly with increasing travel time, reaching stable levels around 400 cm^{-3} and below beyond travel times of 24 hours. To make this result useful for other studies aimed at minimizing the continental influence on the marine atmosphere we fitted a combination of rapid exponential and slow linear decay to N_3 in Figure S6. Eq. 1 shows the respective decay formula with t being the trajectory travel time in hours from the nearest continent.

$$N_3 = 4594 * e^{(-0.178*t)} - 0.6512 * t + 374.03 \quad (1)$$

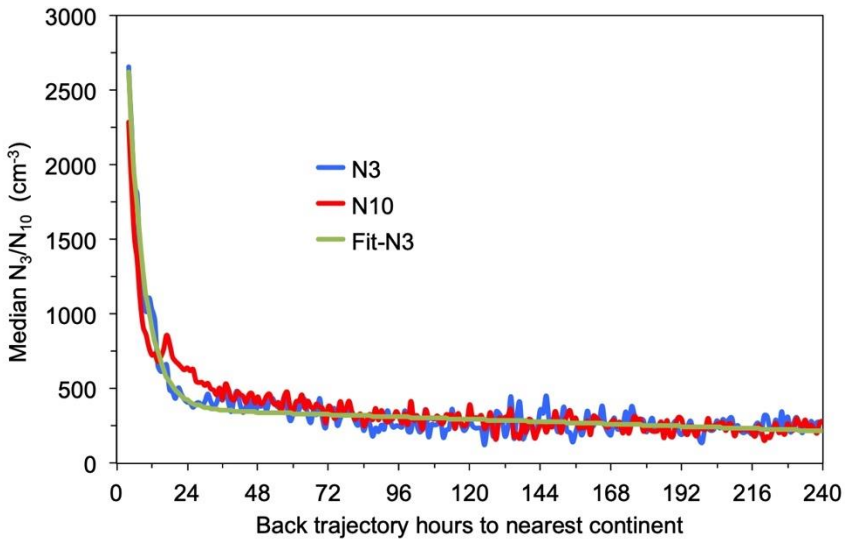

Figure S6 Median N_3 and N_{10} (cm^{-3}) at all stations and on all cruises as function of back trajectory hours to the nearest continent. Fit-N3 = A sum of an exponential and a linear decay fitted to N_3, see text for details.

A second test was made with the hourly N_{10} data from Kennaook Cape Grim along with ^{222}Radon data during the years 1989-2002. The measurement of ^{222}Rn has proven to be an excellent indicator of the continental nature of air sampled in marine environments because it is almost exclusively of continental origin (Larson and Bressan, 1980). At Kennaook Cape Grim this measurement was established by Whittlestone in the 1980s, (Whittlestone, 1989). For the years 1989 to 2002 hourly Rn data were available for the present study along with hourly particle number concentrations and major ion data. At Cape Point complementary ^{222}Rn was available for the CN data during 2008-2012. Whenever possible the procedures discussed above were applied to the physical and chemical aerosol data to filter out potential continental influences. Independent of the locally determined filtering procedures discussed in this section the constraint of at least five days of back trajectories to the nearest continent was applied to all data discussed below, except for MSA, (cf. section 3.2.1 in the manuscript).

Figure S7 shows median N_{10} and Radon as function of travel time to the nearest continent. Both, ^{222}Radon and N_{10} drop rapidly with travel time with levelling out after about 48 hours with N_{10} around 300 cm^{-3}. We deduce from these results that the threshold of 100 $mBqm^{-3}$ as

threshold in segregating Kennaook Cape Grim data with minimum continental influence reported by Zahorowski et al., (1996) was well justified. At times without Radon information a threshold of 48h of travel time from Australia was used.

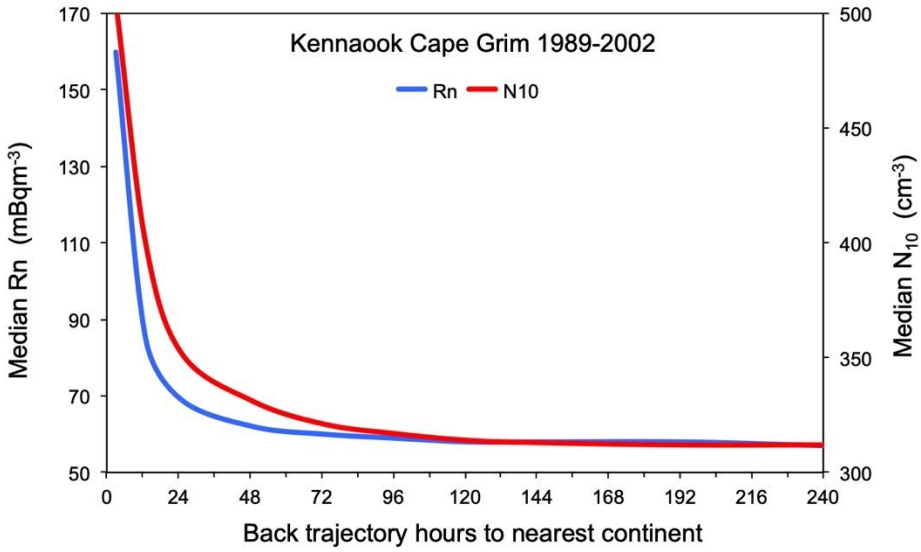

Figure S7 Median N_{10} (N10, cm^{-3}), and ^{222}Radon (Rn, $mBqm^{-3}$) at Kennaook Cape Grim, Tasmania during the years 1989 – 2002 as function of back trajectory hours to the nearest continent.

It would be desirable to conduct comparable contamination exercises at all other stations and on the cruises of the present study. However, the necessary tracer data were not available.

Literature

Asmi, E., Frey, A., Virkkula, A., M, E., Manninen, H. and co-authors 2010. Hygroscopicity and chemical composition of Antarctic sub-micrometre aerosol particles and observations of new particle formation. *Atmos. Chem. Phys.* **10**.

Asmi, E., Neitola, K., Teinilä, K., Rodriguez, E., Virkkula, A. and co-authors 2018. Primary sources control the variability of aerosol optical properties in the Antarctic Peninsula. *Tellus B* **70**, 1-16.

188 Ayers, G. 2001. Influence of local soil dust on composition of aerosol samples at Cape Grim.
189 In: *Baseline Atmospheric Program Australia 1997-98* eds. Tindale, N. W., N. Derek
190 and R. J. Francey). Bureau of Meteorology and CSIRO Atmospheric Research,
191 Melbourne, Australia, 50-56.
192 Ayers, G. P., Cainey, J. M., Granek, H. and Leck, C. 1996. Dimethylsulfide oxidation and the
193 ratio of methansulfonate to non sea-salt sulfate in the marine aerosol. *J. Atmos. Chem.*
194 **25**, 307-325.
195 Ayers, G. P., Cainey, J. M., Gillett, R. W. and Ivey, J. P. 1997. Atmospheric sulphur and
196 cloud condensation nuclei in marine air in the Southern Hemisphere. *Philos Trans R*
197 *Soc Lond B Biol Sci* **352**, 203-211.
198 Ayers, G. P. and Gillett, R. W. 2000. DMS and its oxidation products in the remote marine
199 atmosphere: implications for climate and atmospheric chemistry. *Journal of Sea*
200 *Research* **43**, 275-286.
201 Bates, T. S., Quinn, P. K., Covert, D. S., Coffman, D. J., Johnson, J. E. and co-authors 2000.
202 Aerosol physical properties and processes in the lower marine boundary layer: A
203 comparison of shipboard sub-micron data from ACE-1 and ACE-2. *Tellus* **52B**, 258-
204 272.
205 Bates, T. S., Quinn, P. K., Coffman, D. J., Johnson, J. E., Miller, T. L. and co-authors 2001.
206 Regional physical and chemical properties of the marine boundary layer aerosol across
207 the Atlantic during AEROSOLS99: An overview. *J. Geophys. Res.* **106**, 20767-20782.
208 Becagli, S., Barbaro, E., Bonamano, S., Caiazzo, L., di Sarra, A. and co-authors 2022. Factors
209 controlling atmospheric DMS and its oxidation products (MSA and nssSO42-) in the
210 aerosol at Terra Nova Bay, Antarctica. *Atmos. Chem. Phys.* **22**, 9245–9263.
211 Brechtel, F. J., Kreidenweis, S. M. and Swan, H. B. 1998. Air mass characteristics, aerosol
212 particle number concentrations and number size distributions at Macquarie Island

during the First Aerosol Characterization Experiment (ACE 1). *J. Geophys. Res.* **103**, 16351-16367.

Claeys, M., Wang, W., Vermeylen, R., Kourtchev, I., Chi, X. and co-authors 2010. Chemical characterisation of marine aerosol at Amsterdam Island during the austral summer of 2006–2007. *J. Aerosol Sci.* **41**, 13-22.

Decesari, S., Paglione, M., Rinaldi, M., Dall'Osto, M., Simó, R. and co-authors 2020. Shipborne measurements of Antarctic submicron organic aerosols: an NMR perspective linking multiple sources and bioregions. *Atmos. Chem. Phys.* **20**, 4193-4207.

Gras, J. L. 1990. Baseline atmospheric condensation nuclei at Cape Grim 1977-1987. *J. Atmos. Chem.* **11**, 89-106.

Gras, J. L. 1995. CN, CCN and particle size in southern ocean air at Cape Grim. *Atmos. Res.* **35**, 233-251.

Hara, K., Sudo, K., Ohnishi, T., Osada, K., Yabuki, M. and co-authors 2019. Seasonal features and origins of carbonaceous aerosols at Syowa Station, coastal Antarctica. *Atmos. Chem. Phys.* **19**, 7817-7837.

Herenz, P., Wex, H., Mangold, A., Laffineur, Q., Gorodetskaya, I. V. and co-authors 2019. CCN measurements at the Princess Elisabeth Antarctica research station during three austral summers. *Atmos. Chem. Phys.* **19**, 275-294.

Hogan, A. W. 1981. Aerosol Measurements Over and Near the South Pacific Ocean and Ross Sea. *Journal of Applied Meteorology (1962-1982)* **20**, 1111-1118.

Hong, S.-b., Yoon, Y. J., Becagli, S., Gim, Y., Chambers, S. D. and co-authors 2020. Seasonality of aerosol chemical composition at King Sejong Station (Antarctic Peninsula) in 2013. *Atmos. Environ.* **223**, 117185.

Huang, S., Wu, Z., Poulain, L., van Pinxteren, M., Merkel, M. and co-authors 2018. Source apportionment of the organic aerosol over the Atlantic Ocean from 53°N to 53°S:

significant contributions from marine emissions and long-range transport. *Atmos. Chem. Phys.* **18**, 18043-18062.

Humphries, R. S., Klekociuk, A. R., Schofield, R., Keywood, M., Ward, J. and co-authors 2016. Unexpectedly high ultrafine aerosol concentrations above East Antarctic sea ice. *Atmos. Chem. Phys.* **16**, 2185-2206.

Humphries, R. S., Keywood, M. D., Gribben, S., McRobert, I. M., Ward, J. P. and co-authors 2021. Southern Ocean latitudinal gradients of Cloud Condensation Nuclei. *Atmos. Chem. Phys. Discuss.* **2021**, 1-35.

Jang, E., Park, K.-T., Yoon, Y. J., Kim, K., Gim, Y. and co-authors 2022. First-year sea ice leads to an increase in dimethyl sulfide-induced particle formation in the Antarctic Peninsula. *Sci. Total Environ.* **803**, 150002.

Jung, J., Hong, S. B., Chen, M., Hur, J., Jiao, L. and co-authors 2020. Characteristics of methanesulfonic acid, non-sea-salt sulfate and organic carbon aerosols over the Amundsen Sea, Antarctica. *Atmos. Chem. Phys.* **20**, 5405-5424.

Kanamitsu, M. 1989. Description of the NMC Global Data Assimilation and Forecast System. *Wea. Forecasting* **4**, 335-342.

Keywood, M. D. 2003. Aerosol Chemistry at Cape Grim. In: *Baseline Atmospheric Program Australia 1999-2000* eds. Tindale, N., N. Derek and P. B. Fraser). Bureau of Meteorology and CSIRO Marine and Atmospheric Research, Melbourne, Australia, 31-41.

Keywood, M. D. 2007. Aerosol composition at Cape Grim: an evaluation of the PM10 sampling program and baseline event switches. In: *Baseline Atmospheric Program Australia 2005-2006* eds. Cainey, J., N. Derek and P. B. Krummel). Australian Bureau of Meteorology and CSIRO Marine and Atmospheric Research, Melbourne, Australia, 31-35.

Koponen, I. K., Virkkula, A., Hillamo, R., Kerminen, V.-M. and Kulmala, M. 2002. Number size distributions and concentrations of marine aerosols: Observations during a cruise between the English Channel and the coast of Antarctica. *J. Geophys. Res.* **107**, 10.1029/2002JD002533.

Kubicki, M., Odzimek, A. and Neska, M. 2016. Relationship of ground-level aerosol concentration and atmospheric electric field at three observation sites in the Arctic, Antarctic and Europe. *Atmos. Res.* **178-179**, 329-346.

Larson, R. E. and Bressan, D. J. 1980. Radon-222 as an indicator of continental air masses and air mass boundaries over ocean areas. In: Proceedings of the Conference on Natural Radiation Environment III, Houston, TX, USA, 1980, http://inis.iaea.org/search/search.aspx?orig_q=RN:12624646.

Leck, C., Heintzenberg, J. and Engardt, M. 2002. A meridional profile of the chemical composition of submicrometer particles over the East Atlantic Ocean: Regional and hemispheric variabilities. *Tellus* **54B**, 377-384.

Legrand, M., Yang, X., Preunkert, S. and Theys, N. 2016. Year-round records of sea salt, gaseous, and particulate inorganic bromine in the atmospheric boundary layer at coastal (Dumont d'Urville) and central (Concordia) East Antarctic sites. *J. Geophys. Res.* **121**, 997-1023.

Legrand, M., Weller, R., Preunkert, S. and Jourdain, B. 2021. Ammonium in Antarctic Aerosol: Marine Biological Activity versus Long-Range Transport of Biomass Burning. *Geophys. Res. Lett.* **48**, e2021GL092826.

Li, J., Michalski, G., Davy, P., Harvey, M., Katzman, T. and co-authors 2018. Investigating Source Contributions of Size-Aggregated Aerosols Collected in Southern Ocean and Baring Head, New Zealand Using Sulfur Isotopes. *Geophysical Research Letters* **45**, 3717-3727.

289 Lubin, D., Zhang, D., Silber, I., Scott, R. C., Kalogeras, P. and co-authors 2020. AWARE:
290 The Atmospheric Radiation Measurement (ARM) West Antarctic Radiation
291 Experiment. *Bull. Amer. Meteor. Soc.* **101**, E1069-E1091.
292 McFarquhar, G. M., Bretherton, C. S., Marchand, R., Protat, A., DeMott, P. J. and co-authors
293 2021. Observations of Clouds, Aerosols, Precipitation, and Surface Radiation over the
294 Southern Ocean: An Overview of CAPRICORN, MARCUS, MICRE, and
295 SOCRATES. *Bull. Amer. Meteor. Soc.* **102**, E894-E928.
296 Neff, P. D. and Bertler, N. A. N. 2015. Trajectory modeling of modern dust transport to the
297 Southern Ocean and Antarctica. *J. Geophys. Res.* **120**, 9303-9322.
298 Ogren, J. A. and Heintzenberg, J. 1990. Parametric aerosol sampling at low concentration
299 levels. Report AA-1, Department of Meteorology, Stockholm University, 11pp.
300 Pant, V., Siingh, D. and Kamra, A. K. 2011. Size distribution of atmospheric aerosols at
301 Maitri, Antarctica. *Atmos. Environ.* **45**, 5138-5149.
302 Prospero, J. M., Savoie, D. L., Saltzman, E. S. and Larsen, R. 1991. Impact of oceanic sources
303 of biogenic sulphur on sulphate aerosol concentrations at Mawson, Antarctica. *Nature*
304 **350**, 221-223.
305 Quinn, P. K., Coffman, D. J., Johnson, J. E., Upchurch, L. M. and Bates, T. S. 2017. Small
306 fraction of marine cloud condensation nuclei made up of sea spray aerosol. *Nature*
307 *Geosci.* **10**, 674-679.
308 Robbins, F. J. and Enting, I. G. 1989. Trajectory analysis of selected CO2 data. II. In:
309 *Baseline Atmospheric Program (Australia)* eds. Forgan, B. W. and G. P. Ayers).
310 CSIRO Division of Atmospheric Reseach, Mordialloc, Australia, 9-15.
311 Sakerin, S. M., Golobokova, L. P., Kabanov, D. M., Khuriganowa, O. I., Pol'kin, V. V. and
312 co-authors 2022. Spatial Distribution of Aerosol Characteristics over the South
313 Atlantic and Southern Ocean Using Multiyear (2004-2021) Measurements from
314 Russian Antarctic Expeditions. *Atmosphere* **13**, 427.

315 Savoie, D. L. 1984. *Nitrate and non-sea-salt sulfate aerosols over major regions of the world*
316 *ocean: concentrations, sources and fluxes*. Ph.D. Department, University of Miami,
317 USA, Miami FL.
318 Savoie, D. L. and Prospero, J. M. 1989. Comparison of oceanic and continental sources of
319 non-sea-salt sulphate over the Pacific Ocean. *Nature* **339**, 685-687.
320 Savoie, D. L., Prospero, J. M., Larsen, R. J. and Saltzman, E. S. 1992. Nitrogen and sulfur
321 species in aerosols at Mawson, Antarctica, and their relationship to natural
322 radionuclides. *J. Atmos. Chem.* **14**, 181-204.
323 Savoie, D. L., Prospero, J. M., Larsen, R. J., Huang, F., Izaguirre, M. A. and co-authors 1993.
324 Nitrogen and sulfur species in Antarctic aerosols at Mawson, Palmer station, and
325 Marsh (King George Island). *J. Atmos. Chem.* **17**, 95-122.
326 Schmale, J., Schneider, J., Nemitz, E., Tang, Y. S., Dragosits, U. and co-authors 2013. Sub-
327 Antarctic marine aerosol: dominant contributions from biogenic sources. *Atmos.*
328 *Chem. Phys.* **13**, 8669-8694.
329 Schmale, J., Baccarini, A., Thurnherr, I., Henning, S., Efraim, A. and co-authors 2019a.
330 Overview of the Antarctic Circumnavigation Expedition: Study of Preindustrial-like
331 Aerosols and Their Climate Effects (ACE-SPACE). *Bull. Amer. Meteor. Soc.* **100**,
332 2260-2283.
333 Schmale, J., Henning, S., Tummon, F., Hartmann, M., Baccarini, A. and co-authors 2019b.
334 Aerosol particle number concentration measured over the Southern Ocean in the
335 austral summer of 2016/2017, during the Antarctic Circumnavigation Expedition. doi:
336 10.5281/zenodo.2636690.
337 Stein, A. F., Draxler, R. R., Rolph, G. D., Stunder, B. J. B., Cohen, M. D. and co-authors
338 2015. NOAA's HYSPLIT Atmospheric Transport and Dispersion Modeling System.
339 *Bull. Amer. Meteor. Soc.* **96**, 2059-2077.

340 Teinilä, K., Kerminen, V.-M. and Hillamo, R. 2000. A study of size-segregated aerosol
341 chemistry in the Antarctic atmosphere. *J. Geophys. Res.* **105**, 3893-3904.
342 Wang, S., Yan, J., Lin, Q., Zhang, M., Xu, S. and co-authors 2021. Formation of marine
343 secondary aerosols in the Southern Ocean, Antarctica. *Environ. Chem.* **18**, 285-293.
344 Weller, R., Wöltjen, J., Piel, C., Resenberg, R., Wagenbach, D. and co-authors 2008. Seasonal
345 variability of crustal and marine trace elements in the aerosol at Neumayer station,
346 Antarctica. *Tellus B* **60**.
347 Weller, R., Minikin, A., Wagenbach, D. and Dreiling, V. 2011a. Characterization of the inter-
348 annual, seasonal, and diurnal variations of condensation particle concentrations at
349 Neumayer, Antarctica. *Atmos. Chem. Phys.* **11**.
350 Weller, R., Wagenbach, D., Legrand, M., Elsässer, C., Tian-Kunze, X. and co-authors 2011b.
351 Continuous 25-yr aerosol records at coastal Antarctica - I: Inter-annual variability of
352 ionic compounds links to climate indices. *Tellus B* **63**, 901-919.
353 Weller, R., Schmidt, K., Teinilä, K. and Hillamo, R. 2015. Natural new particle formation at
354 the coastal Antarctic site Neumayer. *Atmos. Chem. Phys.* **15**, 11399-11410.
355 Whittlestone, S. 1989. Radon daughter disequilibria in the lower marine boundary layer. *J.*
356 *Atmos. Chem.* **8**, 16pp.
357 Xu, G., Chen, L., Zhang, M., Zhang, Y., Wang, J. and co-authors 2019. Year-round records of
358 bulk aerosol composition over the Zhongshan Station, Coastal East Antarctica. *Air*
359 *Quality, Atmosphere & Health* **12**, 271-288.
360 Yan, J., Jung, J., Lin, Q., Zhang, M., Xu, S. and co-authors 2020. Effect of sea ice retreat on
361 marine aerosol emissions in the Southern Ocean, Antarctica. *Sci. Total Environ.* **745**,
362 140773.
363 Zahorowski, W., Galbally, I. E., Whittlestone, S. and Meyer, C. P. 1996. Ozone and Radon at
364 Cape Grim: A study of their interdependence. In: *Baseline Atmospheric Program*
365 *(Australia) 1993* eds. Francey, R. J., A. L. Dick and N. Derek). Department of the

Environment, Sport and Territories, Bureau of Meteorology in cooperation with CSIRO Division of Atmospheric Research, Melbourne, Australia, 30-38.

Zhang, M. M., Marandino, C. A., Yan, J. P., Lin, Q., Park, K. and co-authors 2021. DMS sea-to-air fluxes and their influence on sulfate aerosols over the Southern Ocean, south-east Indian Ocean and north-west Pacific Ocean. *Environ. Chem.*

Zorn, S. R., Drewnick, F., Schott, M., Hoffmann, T. and Borrmann, S. 2008. Characterization of the South Atlantic marine boundary layer aerosol using an aerodyne aerosol mass spectrometer. *Atmos. Chem. Phys.* **8**, 4711-4728.